

Meral Turabık¹
 Belgin Gozmen²

¹Technical Science Vocational School,
 Chemical Prog., Mersin University,
 Mersin, Turkey

²Department of Chemistry, Arts and
 Sciences Faculty, Mersin University,
 Mersin, Turkey

Research Article

Removal of Basic Textile Dyes in Single and Multi-Dye Solutions by Adsorption: Statistical Optimization and Equilibrium Isotherm Studies

The removal of three basic dyes by adsorption onto bentonite was investigated for single, binary, and ternary solutions in a batch system. Before and after dye adsorption, bentonite samples were analyzed by using X-ray fluorescence spectrometer, SEM, and Fourier transform IR spectrometry. The D-optimal design and response surface methodology were applied in designing the experiments for evaluating the interactive effects of each initial concentrations variable of the dyes in binary systems. Predicted values were found to be in good agreement with experimental values, which defined propriety of the model and the achievement of D-optimal in optimization of adsorption of binary dye systems. The competitive adsorption results showed that the adsorption amount of a dye was suppressed in the presence and increasing concentrations of second or third dye. For mono-component isotherm modeling, Langmuir and Freundlich models were applied to equilibrium data of single, binary, and ternary dye solutions, while modified Langmuir, Sheindrof-Rebhun-Sheintuch and modified extended Freundlich models were also applied to equilibrium data of binary dye solutions for multi-component isotherm modeling. The results showed that the Langmuir was the more suitable model for single dye systems while extended Freundlich model fitted best to the experimental data with the lowest error values for multi-dye systems.

Keywords: Bentonite; Multi-component adsorption; Pollution; Response surface methodology; Wastewater treatment

Received: May 15, 2012; *revised:* September 6, 2012; *accepted:* September 30, 2012

DOI: 10.1002/clean.201200220

1 Introduction

One of the main resources of environmental pollution is dye-containing wastewaters which arises by the dye production and its use in the textile and other industries [1]. These wastewaters may be fairly colored, highly toxic to aquatic biota, and affect the natural equilibrium because of the reducing effect of photosynthetic activity [2]. Dyes can be classified as basic, acid, disperse, azo, diazo, metal complex, and anthraquinone based. The reasons for that bright, soluble and high tinctorial value increase the use of basic dyes in textile industry [3]. Because of the variety of dyes employed in the dyeing processes and, has a synthetic origin and complex structure, it is difficult to completely remove all types of dyes in wastewaters [3, 4]. One of the most effective techniques for removal of dyes from such wastewater is adsorption by activated carbon but it is expensive [5]. Thus, the use of low-cost adsorbents has been investigated.

Bentonite, which is predominantly montmorillonite clay, is 2:1-type aluminosilicate. At silica tetrahedral (T), Si⁴⁺ is in tetrahedral coordination with O²⁻ while at the alumina octahedral (O), Al³⁺ in octahedral coordination with O²⁻. The tetrahedral and octahedral are interconnected by the sharing of O²⁻ at polyhedral corners and edges. Thus, bentonite is characterized as T-O-T composition by one alumina octahedral sheet placed between two silica tetrahedral sheets. By the results of an isomorphous partial substitution of Al³⁺ in octahedral sites by Mg²⁺ and Fe²⁺/Fe³⁺ and to a lesser degree and partial substitution of Si⁴⁺ in tetrahedral sites by Al³⁺, a net negative surface charge and interlayer space between T-O-T layers are obtained on the bentonite. This charge imbalance is offset by exchangeable cations such as Na⁺, K⁺, Ca²⁺ to neutralize the charge at the bentonite surface [6, 7]. When the negatively charged particles mixed with a solution containing cations, these cations is to be directed towards the surface of the particles, and then either neutral or charged complexes will be formed from the binding of mono-valent sites [8, 9]. In recent years, clay minerals have taken into consideration as important adsorbents due to their high surface area, high cation exchange capacity (CEC), and high chemical and mechanical stabilities [10, 11]. The adsorption of dyes by clay in single component solutions has been studied amply, however, there are relatively few adsorption studies for multi-component systems studied with clays and also much of the work intensified especially

Correspondence: Dr. M. Turabık, Technical Science Vocational School, Chemical Prog., Mersin University, 33343 Mersin, Turkey
 E-mail: mturabik@mersin.edu.tr

Abbreviations: ANOVA, analysis of variance; BB, basic blue; BR, basic red; BY, basic yellow; RSM, response surface methodology; SRS, Sheindrof-Rebhun-Sheintuch

for heavy metal removal using different adsorbents in multi-component system [12–18].

Generally, textile industry wastewaters contain more than one dye as pollutant. The results of some investigations show that a competition take place in multi-dye solutions between dyes for the active sites of adsorbents [1, 3, 13, 16, 17, 19, 20]. Adsorption capacity of some adsorbents may decrease because of the interactions between dyestuffs. In this competitive adsorption system, incorrect results may be obtained by evaluating the experimental data by using known mono-component adsorption models. Thus, the evaluation of multi-component sorption equilibrium is also a complex problem for the competitive adsorption processes [21].

Understanding of multi-dye interaction with bentonite would be very helpful for its use in wastewater treatment. Moreover, statistical analysis and equilibrium studies are highly important to optimize the design of adsorption processes. For these reasons, firstly the removal of basic dyes in single, binary, and ternary solutions by

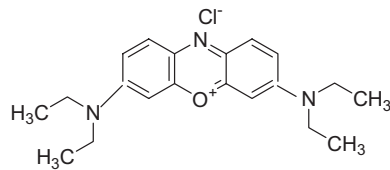
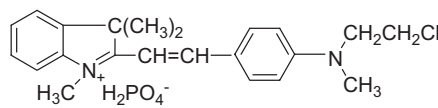
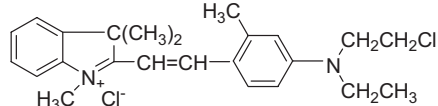
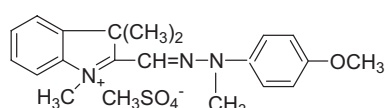
adsorption onto bentonite was investigated and then adsorption equilibriums were studied. And, also response surface methodology (RSM) was applied to obtained data to evaluate the performance of adsorption capacity of bentonite for binary dye solutions depending on the initial dye concentrations. RSM is an effective tool for the statistical design of experiments that is primarily used to evaluate the simultaneous effect of operating conditions or to search optimum conditions for desirable responses [22].

2 Materials and methods

2.1 Materials

Astrazon Blue BG micro 200% (Basic Blue, BB), Astrazon BrRed B 200%01 (Basic Red, BR), Astrazon GldYellow GL-E 400% (Basic Yellow, BY) textile dyes were supplied by DyStar Textile firm. The chemical structures and safety data sheet of these dyes in accordance with the EU Directives [23] are given in Table 1.

Table 1. The chemical structures and safety data sheet of dyes in accordance with the EU Directives [23]

Color index number/dye composition, commercial names, and chemical structure	MW (g/mol)	Biodegradability	COD (mg/g)	pH (100 g/L)	Hazard symbols*
BB C.I. Basic Blue 3/50-55% Astron Blue BG micro 200%	359.89	<10%	830	4.5–5.5	T, N, R23/25-41-50/53
					
BR Astrazon BrRed B 200/0.1% C.I. Basic Red 13-phosphate/35-45%	403.43	<10%	1490	2.0–2.5	Xn, N, R22-41-50/53
					
C.I. Basic Violet 7/50-60%	405.40				
					
BY C.I. Basic Yellow 28/85-95% Astron Gld Yellow GL-E 400%	421.51	<10%	2000	5.0–7.0	Xn, N, R22-41-50/53
					

* T, toxic; N, dangerous for the environment; Xn, harmful; R22, harmful if swallowed; R41, risk of serious damage to eyes; R23/25, toxic by inhalation and if swallowed; R50/53, very toxic to aquatic organisms, may cause long term adverse effects in the aquatic environment.

The Unye/Ordu bentonite used as an adsorbent was crushed, ground, and sieved through a 75- μm sieve. The mineral phase of bentonite was determined as predominantly montmorillonite, the specific surface area and CEC of bentonite were also determined as 72.5 m²/g and 0.992 meq/g, respectively in previous research of Turabik and Kumbur [24]. Before and after the adsorption, bentonite samples were analyzed at Fourier transform IR spectrometry (FTIR), X-ray fluorescence (XRF) spectrometer, and SEM. For this purpose, a suspension was prepared by adding 20 g of bentonite to 2000 mg/L of dyes solutions. The suspensions were continuously stirred by a magnetic stirrer for 2 h. Then the bentonite particles were sedimented, separated from the dye solution, and the water was evaporated at 105°C for 24 h.

FTIR analysis of dyes and bentonite, before and after dye adsorption, was recorded using a Perkin Elmer Model FTIR Frontier spectrophotometer with attenuated total reflection (ATR) technique in the 4000–450/cm region. The bentonite and dye adsorbed bentonite were brought to constant weight in a drying oven at 105°C for 24 h. A Rigaku ZSX Primus II model XRF by dispersive energy spectrophotometer was used to determine qualitatively and semi quantitatively (SQX program) the elements present in the bentonite and dye adsorbed bentonite samples.

SEM analysis was performed by mounting bentonite samples onto pin type SEM stubs using carbon adhesive tabs and was coated with carbon by electrodeposition under vacuum prior to analysis to enhance the surface conductivity. The bentonite and dye adsorbed bentonite samples were examined on a Zeiss/Supra 55 field emission SEM.

2.2 Dyes and analysis

The stock solutions of BB, BR, and BY dyes were prepared in 1.0 g/L concentration. For further experiments, the necessary dilute solutions were prepared from these stock solutions of each dye. The initial pH of each solution was adjusted to pH 6.0 before mixing with bentonite. Shimadzu UV-160A spectrophotometer was used for spectrophotometric analysis of studied dyes. The zero and first order derivative spectra's were used for the analysis of dyes remaining in single and multi-dye solutions, respectively.

2.3 Batch adsorption studies

0.1 g of bentonite was mixed with 100 mL of single or multi dye solutions of BB, BR, and BY in an Erlenmeyer flask as a batch system. The concentration ratios of dyes were always maintained at 1:1 w/w and 1:1:1 w/w/w in equilibrium studies for binary and ternary dye solutions, respectively. The studies to determine optimum pH and temperature showed that temperature slightly affects the adsorption and also pH-independent process (data not shown). The similar results were obtained by Eren and Afsin [25] for the cationic dyes adsorption onto bentonite. Thus, dye solutions were agitated by using a shaker at 30°C, pH 6.0 and 100 rpm. After 2 h, adsorption equilibrium was established. Samples were taken both initial dye solutions and end of the 2 h. These samples were centrifuged at 3500 rpm for 10 min, and then dye containing of supernatants were analyzed spectrophotometrically.

The adsorbed amount of each dye per unit weight of adsorbent at equilibrium, $q_{\text{eq},i}$ (mg dye/g adsorbent) and dye removal (%) can be

calculated by using Eqs. (1) and (2), respectively.

$$q_{\text{eq},i} = \frac{(C_{0,i} - C_{\text{eq},i})V}{w} \quad (1)$$

$$\text{Remove of "i" component \%} = \frac{100(C_{0,i} - C_{\text{eq},i})}{C_{0,i}} \quad (2)$$

where w is the mass of the adsorbent (g) and V is the volume of dye containing solution (L).

2.4 Experimental design and optimization

In this study, RSM was used for optimization of process variables to enhance the adsorption of binary dye solutions onto bentonite combined with D-optimal design. D-optimal design that chooses runs, often from a larger candidate set of points, based on the D-optimal criterion [26].

Two critical parameters affecting adsorption of binary dye solutions on the bentonite: initial concentration of dye 1 (x_1) and initial concentration of dye 2 (x_2) were selected as independent variables based on preliminary experiments, and the adsorbed amounts of each dye per unit weight of adsorbent at equilibrium, $q_{\text{eq},i}$ were considered as the dependent variables (responses). Experimental results were analyzed using Design Expert 8.1 and regression model was proposed. The real values of independent variables (200, 250, 300, 350 mg/L) were coded as -1 , -0.3 , $+0.3$, and $+1$, respectively. In this study, total 16 experiments for each binary dye solutions were performed in randomized order as required in many design procedures. The D-optimal designed experiments were carried out with six replications in order to evaluate the pure error. The analysis of variance (ANOVA) was used to realize the diagnostic checking tests for adequacy of proposed model, which based on the Fisher's 'F' test. The coefficient of determination, R^2 , is a measure of the amount of variation around the mean explained by the model [27]. By using linear or quadratic models, the responses can be related to chosen factors at an optimization process. A quadratic model can be shown as:

$$Y = \beta_0 + \sum_{j=1}^k \beta_j x_j + \sum_{j=1}^k \beta_{jj} x_j^2 + \sum_{i=1}^k \sum_{<j=2}^k \beta_{ij} x_i x_j + e_i \quad (3)$$

where Y is the response, k is the number of factors, x_i and x_j are the coded variables, β_0 is the offset term, β_j , β_{jj} , and β_{ij} are the first-order, quadratic, and interaction effects, respectively, i and j are the index numbers for factor, and e_i is the residual error [28].

3 Results and discussion

3.1 Simultaneous analysis of BY, BR, and BB in single, binary, and ternary solutions

The zero order absorption spectra of BY, BR, and BB dyes in their single solutions were recorded and maximum wavelength (λ_{max}) of these dyes determined as 437, 531, and 654 nm, respectively (Fig. 1a). The calibration curves were prepared at λ_{max} of each dye. For the initial concentration of 10 mg/L of BY, BR, and BB dyes both in single and ternary solutions, it was expected to obtain same absorbance values at the λ_{max} of each dye but not obtained. The absorption spectra of each dye in binary and ternary solution overlapped. The interferences, which occurred in binary and ternary

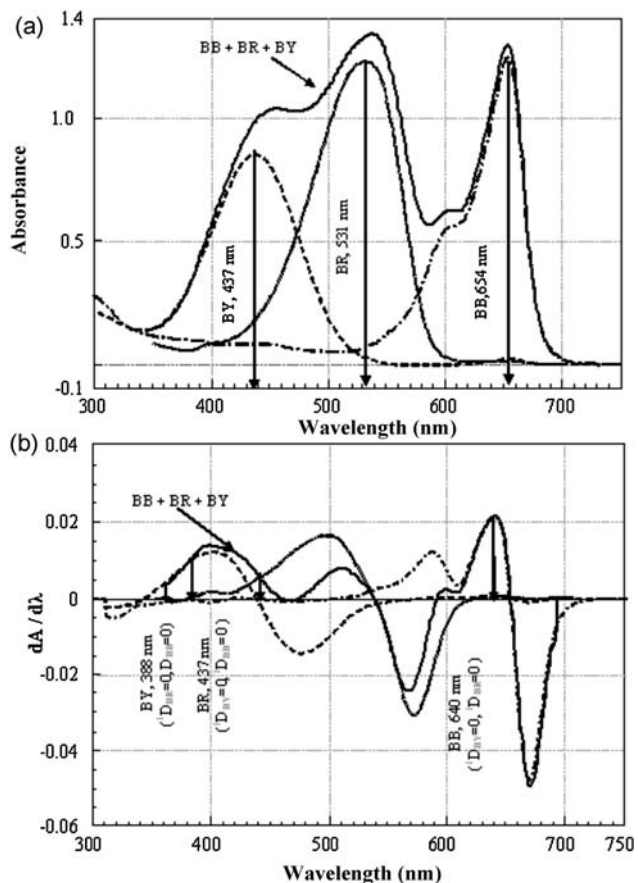


Figure 1. Absorption spectra of BB, BR, and BY in single and ternary solutions (initial dyes concentrations: 10 mg/L); (a) zero order absorption spectra, (b) first order derivative spectra.

solutions caused to changes on the λ_{max} of each dye. For that reason, it is not possible to determine the concentration of each dye in their binary and ternary solutions correctly. Overlapped signals can be separated by means of derivatization of zero order spectrums, thus spectral background interferences effect can be reduced [29]. The first order derivative absorption spectrum can also be obtained by taking the first derivative of the zero order absorbance as a function of wavelength [30]. The variations of first order derivative absorption spectra of BY, BR, and BB in single and ternary solution with wavelength were given in Fig. 1b. It can be seen from Fig. 1b that simultaneous analysis of BY, BR, and BB both in binary and ternary solutions can be determined at 388 nm ($^1D_{BR} = 0, ^1D_{BB} = 0$), 437 nm ($^1D_{BY} = 0, ^1D_{BB} = 0$), 640 nm ($^1D_{BY} = 0, ^1D_{BR} = 0$), respectively. Here, D is the absorbance value of dyes at the first order derivative wavelength. For binary and ternary dye systems, the calibration curves for BY, BR, and BB dyes were prepared at 388 nm ($^1D_{388}$), 437 nm ($^1D_{437}$), and 640 nm ($^1D_{640}$), respectively.

3.2 XRF, FTIR, SEM analysis of bentonite before and after dye adsorption

Major elements of bentonite, before and after BY, BR, and BB dyes adsorption were determined XRF spectrometer. Compositions of the bentonite samples are presented in Table 2. As expected, the adsorp-

Table 2. XRF results of bentonite before and after dye adsorption

Chemical composition%	Bentonite samples	BB adsorbed bentonite	BR adsorbed bentonite	BY adsorbed bentonite
Na ₂ O	1.035	0.604	0.517	0.471
MgO	2.833	2.491	2.510	2.659
Al ₂ O ₃	14.437	13.447	13.094	13.642
SiO ₂	68.463	68.463	68.191	68.826
K ₂ O	0.953	0.906	0.842	0.884
CaO	1.434	1.252	1.193	1.261
Fe ₂ O ₃	1.198	1.157	1.143	1.150
P ₂ O ₅	0.008	0.008	0.142	0.008
SO ₃	0.084	0.054	0.084	0.222
TiO ₂	0.153	0.184	0.151	0.144
LOI	9.2	13.8	16.6	14.2

LOI, loss ignition.

tion process does not effect the crystal structure of the bentonite. Before and after adsorption, when the chemical compositions of the bentonite samples are evaluated, it is seen that the SiO₂ is the same percentage for all samples. But the exchangeable cations percentage, like Na⁺, K⁺, Ca²⁺, Al³⁺, Fe³⁺, are decrease after adsorption. These results imply that the dyes cations exchanges with the bentonite's cations by the adsorption process.

Scanning electron micrographs of bentonite samples were taken before and after dye adsorption (Fig. 2a-d). The SEM of bentonite (Fig. 2a) showed that bentonite had typical sheet-like structure, and different size grains. These lamellas show irregular form. After BY, BR, and BB dyes adsorption the SEM images (Fig. 2b-d) clearly show that dye adsorbed bentonite surface coated by dye molecules and the surfaces of the samples much more homogenous than before adsorption, thus the outstanding lamellar appearance of bentonite become less after the adsorption.

IR techniques have been used by previous researchers for identification of soil and clay minerals [31, 32]. For the adsorption studies, FTIR results can give an idea about the nature of adsorption between

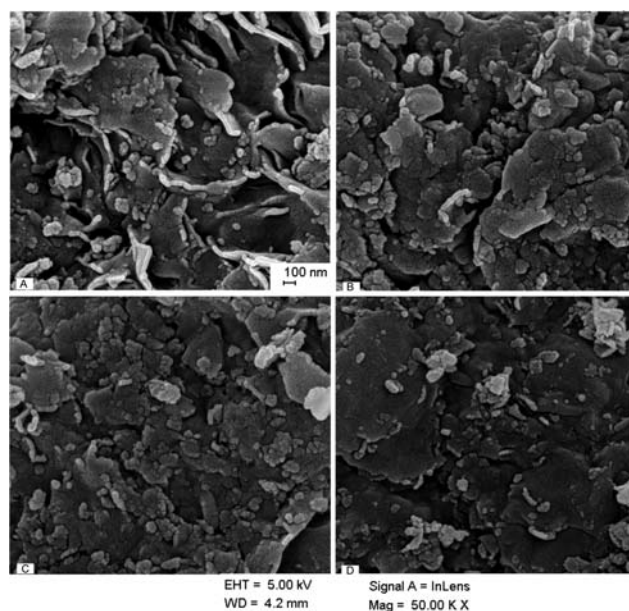


Figure 2. FTIR spectra of bentonite before and after BR dye adsorption.

the adsorbate and adsorbent. The FTIR spectra of bentonite before and after dye adsorption are shown in Fig. 3a–c. Before adsorption, the broad band at around 3624/cm is due to the O–H stretching bands [(Si, Al, Mg)–OH] from the solid. The spectral bands at 1637/cm refer to bending vibration H–OH bond of interlayer water molecules. The strong band at 1015/cm assigned to Si–O stretching vibration of Si–O–Si tetrahedron. At 916, 847, and 795/cm absorption peaks, which were due to stretching band of the Al–Al–OH, Al–Fe–OH [6] and Al–Mg–OH, respectively, indicating the initial layered silicate structure [33]. The other bands around 795, 520, and 467/cm are characteristic absorption bands of a bentonite which is predominantly a montmorillonite clay, which assigned to the Si–O vibrations of quartz impurities, the angular deformation of Si–O–Al bending, and angular deformation of Si–O–Si, respectively [32].

As can be seen in Fig. 3a–c, the spectra of BB, BY, and BR dye are similar and complex. Before and after the adsorption, when the spectra of bentonite and dyes were compared with each other, it was seen that the absorption band of dyes between 500 and 1500/cm overlapped with the absorption spectra of bentonite, thus it was difficult to discuss these area after the dyes adsorption. But, for three dyes, the absorption bands extended between 2960 and 2850/cm are attributed to the C–H asymmetric and symmetric stretching vibration of dye disappear after the adsorption of dyes on bentonite which are masked due to the weak intensity of this vibrations by the bentonite vibrational modes. At the spectrum of BR adsorbed bentonite sample, 1637/cm is attributed to the C=C (not conjugated) stretching vibration of dye. Moreover, the absorptions between 1600 and 1450/cm are typical C=C ring stretches. Similar results were obtained for the FTIR spectra of BB and BY adsorption onto bentonite.

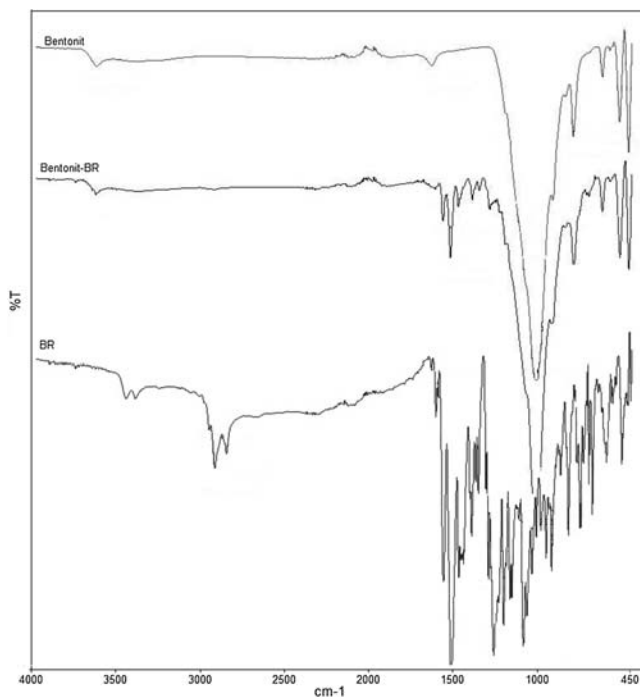


Figure 3. SEM images of bentonite before and after dye adsorption (a) bentonite, (b) BY adsorbed bentonite, (c) BR adsorbed bentonite, and (d) BB adsorbed bentonite.

3.3 The single, binary, and ternary adsorption of dyes

The single and binary adsorption of BY, BR, and BB onto bentonite was investigated in the absence (single dye system) and in the presence of the other dye (BY–BB, BY–BR, BR–BB binary dye system) and compared with each other. For all binary dye system, while the initial first dye concentration value was changed in the range of 200–350 mg/L the initial second dye concentration was held at 0, 200, 250, 300, and 350 mg/L for each run at pH 6.0 and 30°C. Then, the same procedure was applied to the other dye by the order of dye changing.

In the binary solutions, effect of increasing initial second dye concentration to the individual adsorbed amounts of first dye was investigated. Dye removal (%) efficiencies for BY, BR, BB dyes at 300 mg/L initial constant dye concentrations in the absence and in the presence of second dye for the range of 200–350 mg/L are given as column graphics in Fig. 4a–c. It can be seen in Fig. 4a that the amount of BB adsorption decreased with increasing concentration of BY. For example, at 300 mg/L of initial constant BB dye concentration, in the presence of initial concentrations of 0, 200, 250, 300, and 350 mg/L of BY (BB–BY binary systems), BB dye removal (%) values were found as 98, 56, 48, 43, and 42%, respectively. Also, the adsorption of BY reduced in the presence of BB. However, the suppression degree of BY to the adsorption of BB was higher than that of BB. The decreasing trends were also found for the other binary dye systems, but not in same values. Figure 4b shows that adsorption amount of BR onto bentonite was suppressed in the presence of different concentration of BY and the competitive effect of BR on BY adsorption was less than that of BY. It is interesting that other dye removal % values decreased with the presence of BY dye in binary systems (BB–BY, BR–BY). Similarly, the presence of BB tended to reduce the adsorption of BR, but, at BB–BR binary dye system, adsorption reduced capacity of BR is higher than that of BB (Fig. 4c).

As a result, the individual adsorbed dye amounts of first dye at equilibrium (q_{eq}) change with the initial second dye concentration in the solutions. For all binary dye systems, equilibrium BB, BR, and BY uptake onto bentonite decreased with the increase in the other initial dye concentration. A competition develops between the first and second dyes for the adsorption sites on the surface of the adsorbent and some sites are occupied by the winner dye. When the whole data was evaluated for BY–BR, BY–BB, BR–BB binary dye systems, the competitive effect of second dye to first dye removal efficiency could be arranged as $BY > BR > BB$ (Fig. 4a–c).

For the competitive adsorption of BY, BR, and BB onto bentonite in ternary solutions, the concentration ratios of dyes were maintained at 1:1:1 w/w/w for the initial concentration range of 100–400 mg/L to obtain equal competition condition. The comparison of equilibrium uptakes of BB, BR, BY as a function of initial dye concentration for single and ternary solutions are given in Fig. 5. The results showed that the equilibrium uptake capacities of each dye are lower for the all concentration range for ternary solutions to those of single solutions (Fig. 5). The question is that which dye is the best dominant or recessive in the competition? The decreasing ratios of equilibrium uptake were 18, 4, and 1% at 100 mg/L and 75, 59, and 48% at 400 mg/L for BB, BR, BY, respectively. It was determined that when the initial concentrations increased, the decreasing ratio of equilibrium uptake increased, but the dye order is same. These results supported that of binary dye system results. Thus, it can

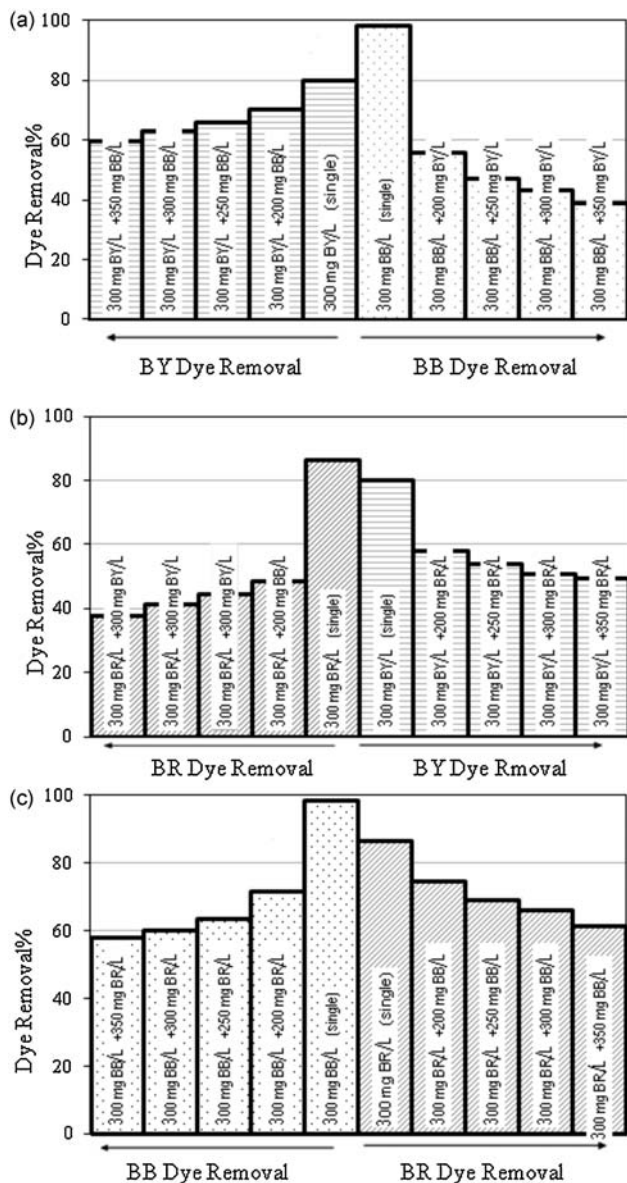


Figure 4. Column graphics of dye removal % efficiencies for BY, BR, BB dyes in the binary solutions for (a) BB–BY, (b) BR–BY, and (c) BB–BR.

be said clearly that the best dominant dye is BY and the best recessive is BB dye in multi-dye solutions.

The application of bentonite as an adsorbent is largely based on its cation exchange property. The ion-exchange capacity of bentonite mostly counts on substitutions within the lattice structure. The inorganic cations on the clay surfaces (e.g. M–O–Na⁺, M–O–K⁺ where M stands for alumina, calcium, silica etc. present in the clay) could be replaced by organic cations. These negative charges are known to be permanent and pH independent [34]. In aqueous solution, cationic dyes, BB, BY, and BR, is the first dissolved Cl⁻, CH₃SO₄⁻, H₂PO₄⁻, and dye-N⁺ groups in their structures. It seemed that all of that had the positive charge on nitrogen atom. There is an electrostatic attraction between the cationic dye-N⁺ groups and the anionic groups in bentonite.

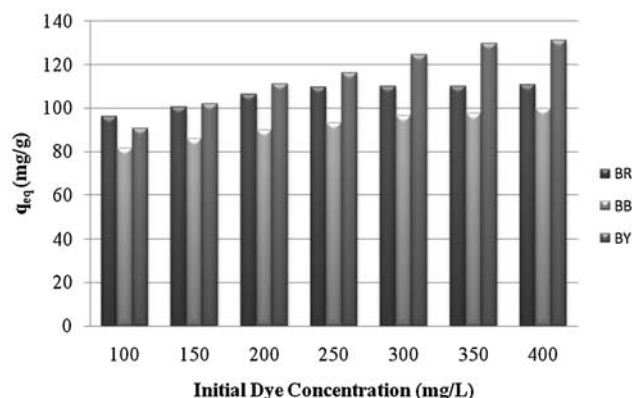
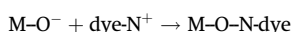


Figure 5. The comparison of equilibrium uptakes of BB, BR, BY as a function of initial dye concentration for single and ternary solutions.

The structures of BR and BY are very similar but BB differs (Table 1). The reason for the BB dye adsorbed more than the others in single solution can be due to the N atom, which carrying a positive charge, encountered less steric hindrance during the approaching functional groups in the structure of clay. When the number of C=C bond increases in molecule, molecular structure of it will have a planar geometry. Due to the phenoxazine structure in the middle of blue dye, this dye has a planar geometry compared to the others and the dye-N⁺ group (N-ethyl-N-methylethanamine) which interacting with the surface of the clay structure, encounter less steric hindrance. Around the N⁺ structure (pyrrolium) onto the BR and BY dyes, there are *cis*- or *trans*-olefin structure (–CH=CH–Ar) and the –CH=N–N–Ar groups. In these dyes, due to these groups, steric blocking will be more. The interaction of dyes onto bentonite took place in the following order of dyes on clay BB > BR > BY.

3.4 RSM analysis

The individual and interactive effects of the selected two variables on the adsorption of the binary dye solutions on the bentonite in an aqueous medium were investigated using the D-optimal design approach. The experimental results were evaluated with RSM of Design-Expert[®] 8. The design used for the optimization and observed responses for 16 experiments are given in Table 3. The ANOVA indicated that the proposed quadratic model could be used for navigating the design space except for total (q_{eq}) for BB–BR binary system. It could be observed that the total (q_{eq}) responses for this binary system fits 2FI model. The approximating functions of the adsorbed amounts of each dye per unit weight of adsorbent at equilibrium, q_{eq,i} (Y) for each binary dye mixture in terms of the coded variables obtained with the D-optimal design are shown as follows:

BY–BB (dye 1–dye 2):

$$Y_{q_{eq}}(BY) = 189.85 + 20.11x_1 - 12.32x_2 + 0.11x_1x_2 - 10.49x_1^2 + 3.06x_2^2$$

$$Y_{q_{eq}}(BB) = 132.12 - 15.77x_1 + 18.65x_2 - 3.98x_1x_2 + 11.60x_1^2 - 5.50x_2^2$$

$$Y_{Total(q_{eq})} = 331.54 + 2.25x_1 + 6.39x_2 - 3.12x_1x_2 - 2.69x_1^2 - 9.29x_2^2$$

Table 3. D-optimal design experiments and experimental results

No.	BY-BB			BY-BR			BB-BR				
	X ₁ C dye 1 (mg/L)	X ₂ C dye 2 (mg/L)	Y ₁ q _{eq} (BY) (mg/g)	Y ₂ q _{eq} (BB) (mg/g)	Y ₃ Total q _{eq} (mg/g)	Y ₁ q _{eq} (BY) (mg/g)	Y ₂ q _{eq} (BR) (mg/g)	Y ₃ Total q _{eq} (mg/g)	Y ₁ q _{eq} (BB) (mg/g)	Y ₂ q _{eq} (BR) (mg/g)	Y ₃ Total q _{eq} (mg/g)
1	200 (-1)	300 (0.33)	157.1	168.9	326.0	146.8	132.1	273.2	141.8	224.3	366.0
2	300(0.33)	200 (-1)	211.6	108.9	320.5	97.6	175.0	280.1	218.9	160.4	373.3
3	200 (-1)	350 (+1)	150.0	175.4	325.4	152.4	123.6	276.1	133.2	232.1	365.3
4	250 (-0.33)	350 (+1)	174.6	150.8	325.4	144.8	139.5	271.0	158.1	210.6	368.7
5	350 (+1)	350 (+1)	193.0	139.0	332.0	126.1	159.6	273.2	178.6	200.3	378.9
6	350 (+1)	350 (+1)	190.5	135.1	325.6	120.3	152.9	262.9	182.4	199.8	382.2
7	350 (+1)	200 (-1)	213.8	106.3	320.1	86.9	182.1	272.6	235.9	153.8	389.7
8	200 (-1)	200 (-1)	173.9	130.2	304.1	112.9	150.0	269.0	161.8	180.6	342.4
9	200 (-1)	350 (+1)	152.0	179.0	331.0	156.7	126.3	285.7	136.0	239.0	375.0
10	300 (0.33)	250 (-0.33)	201.0	125.0	326.0	114.2	167.3	278.9	191.1	181.7	372.8
11	350 (+1)	200 (-1)	211.0	104.0	315.0	80.6	178.6	270.1	231.0	154.6	385.6
12	350 (+1)	350 (+1)	189.0	130.0	319.0	122.8	157.3	259.2	182.9	204.8	387.7
13	300 (0.33)	250 (-0.33)	204.1	127.0	331.0	111.8	164.3	276.0	193.5	184.3	377.8
14	200 (-1)	250 (-0.33)	166.7	159.8	326.5	130.5	139.6	283.0	149.1	217.2	366.3
15	200 (-1)	200 (-1)	175.0	133.1	308.0	115.0	156.0	281.5	164.0	185.0	349.0
16	250 (-0.33)	200 (-1)	196.2	119.0	315.2	106.5	166.7	284.3	200.1	162.5	362.6

BY-BR (dye 1-dye 2):

$$Y_{q_{eq}}(BY) = 125.73 - 15.40x_1 + 19.77x_2 - 0.41x_1x_2 - 2.27x_1^2 - 4.54x_2^2$$

$$Y_{q_{eq}}(BR) = 156.36 + 14.92x_1 - 12.91x_2 + 1.04x_1x_2 - 5.27x_1^2 + 2.49x_2^2$$

$$Y_{Total(q_{eq})} = 282.09 - 0.48x_1 + 6.86x_2 + 0.64x_1x_2 - 7.54x_1^2 - 2.05x_2^2$$

BB-BR (dye 1-dye 2):

$$Y_{q_{eq}}(BB) = 178.17 + 28.27x_1 - 20.45x_2 - 5.77x_1x_2 - 8.26x_1^2 + 8.92x_2^2$$

$$Y_{q_{eq}}(BR) = 196.24 - 15.17x_1 + 23.98x_2 - 1.07x_1x_2 + 10.77x_1^2 - 13.42x_2^2$$

$$Y_{Total(q_{eq})} = 372.70 + 12.58x_1 + 3.64x_2 - 6.78x_1x_2$$

where x_1 and x_2 are corresponding to independent variables of dye 1 and dye 2 concentrations (mg/L), respectively.

ANOVA results of quadratic models are shown in Table 4 for adsorption of binary dye solutions onto bentonite. The quadratic regression models for BY-BB, BY-BR, and BB-BR binary systems were highly significant as the *F*-test (*F*-value) with a very low probability value (*p*-value < 0.0001). Adequate precision is a measure of the experimental signal to noise ratio. This ratio must be >4. Therefore, in the quadratic models adsorption of binary dyes solution onto bentonite, adequate precisions indicate an adequate signal for adsorption process. Based on the ANOVA results, model *F*-Value and associated probability value to confirm model significance. In this study, higher R^2 and adjusted R^2 values obtained. It was explicated that there is a high correlation between the observed values and predicted values [35–39].

The competitive adsorption of BB, BR, and BY dyes was investigated in binary solution in this study by RSM. Initial concentration of dye 1 (x_1) and initial concentration of dye 2 (x_2) were selected as independent variables based on preliminary experiments, and the adsorbed amounts of each dye per unit weight of adsorbent at equilibrium, $q_{eq,i}$ were considered as the dependent variables (responses) at constant pH 6.0, temperature 30°C and time. In Fig. 6, the effects of initial concentration of each dye for binary dye mixture on q_{eq} were shown.

Figure 5a–c shows the effect of initial concentration of two dyes on the adsorption of the binary system for one or both dye. In Fig. 6a and b, it could be observed that the amount of BB adsorption decreased with increasing concentration of BY or vice versa. For BB-BY binary mixture when BB concentration is kept in the highest but BY concentration is kept in the lowest, the maximum value of q_{eq} (BB) was obtained as 175 mg/g (Fig. 6a). In the opposite case, BB concentration is kept in the lowest but BY concentration is kept in the highest, the maximum q_{eq} (BY) was obtained with 213 mg/g (Fig. 6a and b). In fact, this result was observed in the same way as the other binary system (Fig. 6c–f). Figure 7a–c shows the regions obtained for the optimal total adsorption in the binary systems. The maximum total(q_{eq}) value was obtained as 332 mg/g, when the concentrations of BY and BB in the range of 260–330 and 275–320 mg/L, respectively. In BY-BR binary system, the maximum total(q_{eq}) area was obtained as 286 mg/g in the range of initial dye concentrations BY and BR are approximately 250–300 and 330–350 mg/L, respectively (Fig. 7b). If concentration of BR passes 370 mg/L, it can be expected total(q_{eq}) value will decrease. Figure 7c shows maximum area of total(q_{eq}) values for BB-BR binary system. While the concentration of BR between 200 and 300 mg/L and the concentration of BB > 320 mg/L, the maximum total(q_{eq}) value was obtained as 380 mg/g. This maximum value shows a linear increase and the decline is not certain where the next begins.

In competitive adsorption of all binary dyes systems, observed a common result that the maximum q_{eq} value for a dye in binary system was obtained in the case of initial concentration of this dye was higher than the other. For all binary systems, despite the use of the same initial concentrations, the highest q_{eq} values was obtained for BB-BR binary dyes system as close to 240 mg/g. For BY-BB and BB-BR binary systems, when compared to q_{eq} values of BB dye, the inhibitory effect of BY dye seems very clearly.

3.5 Equilibrium of adsorption

Because of the solute-surface interaction and competition of components with each other, multi-component adsorption systems can be complex than in mono-component [18]. Multi-component

Table 4. ANOVA regression model for binary systems

Binary System	Source	Sum of squares	Deg. of freedom	Mean square	F-value	p-value	R ² -values and Adeq. precision
BY-BB	q _{eq} (BY)						
	Model	6799.84	5	1359.97	555.19	<0.0001	R ² = 0.9964
	Residual	24.50	10	2.45			R ² _{adj} = 0.9948
	Lack of fit	5.30	4	1.33	0.41	0.7933	Adeq. prec. = 64.52
	Pure error	19.19	6	3.20			
	q _{eq} (BB)						
	Model	8369.72	5	1673.94	159.94	<0.0001	R ² = 0.9876
	Residual	104.66	10	10.47			R ² _{adj} = 0.9815
	Lack of fit	48.88	4	12.22	1.31	0.3636	Adeq. prec. = 35.39
	Pure error	55.79	6	9.30			
	Total q _{eq}						
	Model	783.31	5	156.66	8.10	0.0027	R ² = 0.8020
Residual	193.44	10	19.34			R ² _{adj} = 0.7029	
Lack of fit	60.14	4	15.04	0.68	0.6324	Adeq. prec. = 7.93	
Pure error	133.30	6	22.22				
BY-BR	q _{eq} (BY)						
	Model	7331.85	5	1466.37	246.20	<0.0001	R ² = 0.9919
	Residual	59.56	10	5.96			R ² _{adj} = 0.9879
	Lack of fit	8.46	4	2.11	0.25	0.9007	Adeq. prec. = 47.07
	Pure error	51.10	6	8.52			
	q _{eq} (BR)						
	Model	4869.35	5	973.87	162.73	<0.0001	R ² = 0.9879
	Residual	59.85	10	5.98			R ² _{adj} = 0.9818
	Lack of fit	4.40	4	1.10	0.12	0.9707	Adeq. prec. = 37.16
	Pure error	55.45	6	9.24			
	Total q _{eq}						
	Model	620.60	5	124.12	5.81	0.0090	R ² = 0.7438
Residual	213.72	10	21.37			R ² _{adj} = 0.6158	
Lack of fit	15.40	4	3.85	0.12	0.9717	Adeq. prec. = 7.59	
Pure error	198.31	6	33.05				
BB-BR	q _{eq} (BB)						
	Model	15436.43	5	3087.29	290.78	<0.0001	R ² = 0.9932
	Residual	106.17	10	10.62			R ² _{adj} = 0.9898
	Lack of fit	73.89	4	18.47	3.43	0.0868	Adeq. prec. = 48.64
	Pure error	32.29	6	5.38			
	q _{eq} (BR)						
	Model	11027.89	5	2205.58	147.68	<0.0001	R ² = 0.9866
	Residual	149.35	10	14.94			R ² _{adj} = 0.9800
	Lack of fit	97.00	4	24.25	2.78	0.1270	Adeq. prec. = 33.16
	Pure error	52.35	6	8.73			
	Total q _{eq}						
	Model-2FI	2297.21	3	765.74	29.35	<0.0001	R ² = 0.8801
Residual	313.09	12	26.09			R ² _{adj} = 0.8501	
Lack of fit	183.83	6	30.64	1.42	0.3399	Adeq. prec. = 15.16	
Pure error	129.26	6	21.54				

systems have received less attention than single component systems. Therefore, the adsorption equilibrium analysis of BY, BR, and BB onto bentonite was investigated not in single systems but also in binary and ternary systems. For single component systems, the Langmuir [40] and Freundlich [41] adsorption isotherm models were applied to equilibrium data. The linear form of the Langmuir isotherm can be represented by Eqs. (4) and (5), respectively.

$$\frac{C_{eq}}{q_{eq}} = \frac{1}{q_{max}K_a} + \frac{C_{eq}}{q_{max}} \quad (4)$$

$$\log q_{eq} = \log K_F + \frac{1}{n} \log C_{eq} \quad (5)$$

where q_{max} (mg/g) and K_a (L/mg) are the Langmuir constants related to monolayer adsorption capacity and energy of adsorption,

respectively. The Freundlich constants K_F [(mg/g) (mg/L)^{1/n}] and $1/n$ are also related to adsorption capacity and intensity of adsorption, respectively.

Individual adsorption constants obtained from the mono-component system may not reflect exactly the multi-component adsorption behavior of dye solutions because of the competition between the components. Some of mono-component equilibrium isotherm equations have been extended or modified for multi-component systems. The multi-component isotherm models, modified Langmuir [42] extended Freundlich [42, 43] and Sheindrof-Rebhun-Sheintuch (SRS) [21] were applied to equilibrium.

Modified Langmuir isotherm model equation can be represented by the following equation:

$$q_{eq,i} = \frac{q_{i,max}K_{a,i}(C_{eq,i}/\eta_i)}{1 + \sum_{j=1}^N K_{a,j}(C_{eq,j}/\eta_j)} \quad (6)$$

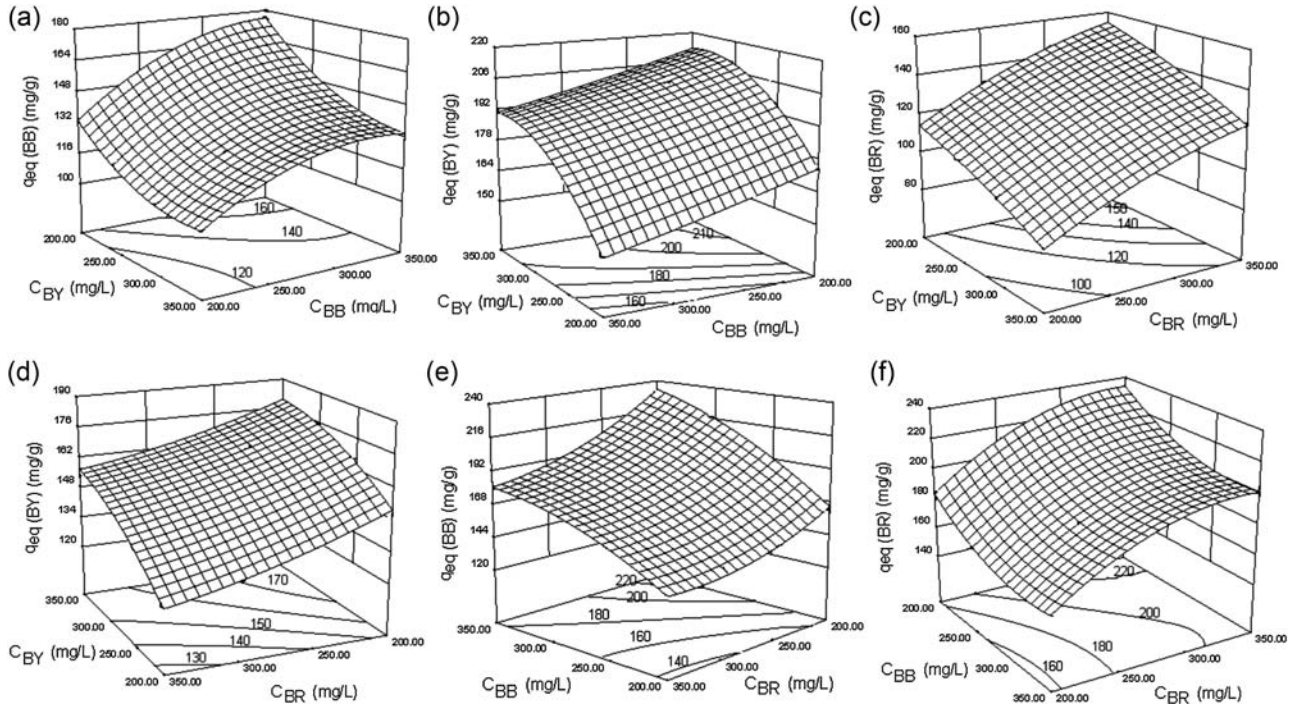


Figure 6. The 3D plot showing effect of initial dye concentrations on adsorption for binary system (a) BB in BB–BY (b) BY in BB–BY (c) BR in BR–BY (d) BY in BR–BY (e) BB in BB–BR (f) BR in BB–BR.

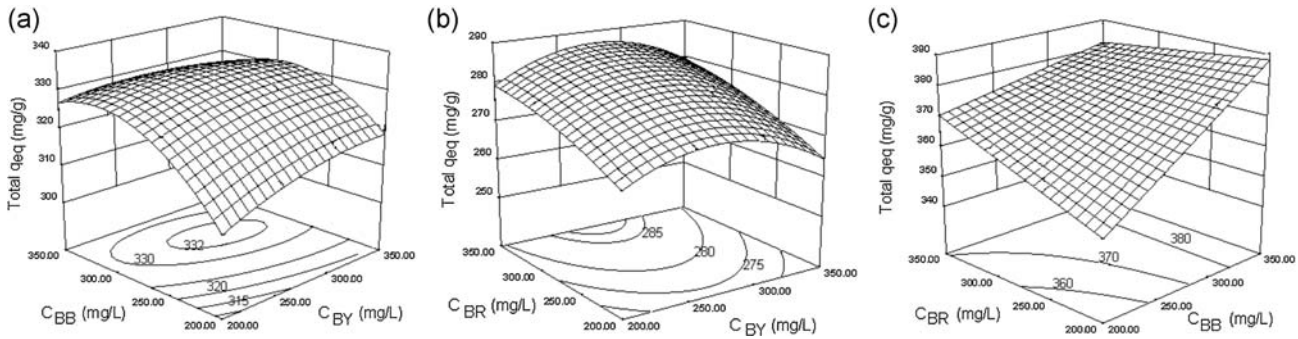


Figure 7. The 3D plot obtained for the optimal total adsorption in the binary systems (a) BY–BB, (b) B–BR, and (c) BR–BB.

where $q_{i,max}$ and $K_{a,i}$ are the Langmuir isotherm parameters obtained from the corresponding individual Langmuir isotherm equations. The parameter, η_i , called as the Langmuir correction coefficient or interaction term is estimated from competitive adsorption data of the ‘i’ component. This parameter is characteristic for each component and its value changing with the presence of the other components.

SRS isotherm model equation can be represented in binary solutions for ‘i’ or ‘j’ component as follows [17]:

$$(q_{eq})_i^j = K_{Fi} C_{\bar{n}} [C_{\bar{n}} + \theta_{ij} C_{\bar{j}}]^{(1/n_i)-1} \quad (7)$$

where $(q_{eq})_i^j$, K_{Fi} and n_i are the equilibrium uptake capacity (mg/g), the single component Freundlich constant and Freundlich exponent for the ‘i’ component in the presence of ‘j’ component, respectively. At this model, the inhibition to the adsorption of component ‘i’ by component ‘j’ is described by the competition coefficient θ_{ij} .

Extended Freundlich isotherm model is valid only for binary solutions, and given by Eqs. (8) and (9) for each component of binary solution.

$$q_{eq1} = \frac{K_{F1} C_{eq1}^{1/(n_1+x_1)}}{C_{eq1}^{x_1+y_1} C_{eq2}^{z_1}} \quad (8)$$

$$q_{eq2} = \frac{K_{F2} C_{eq2}^{1/(n_2+x_2)}}{C_{eq2}^{x_2+y_2} C_{eq1}^{z_2}} \quad (9)$$

The constants of the first and second components in binary solution parameters x_1 ; y_1 ; z_1 and x_2 ; y_2 ; z_2 are described as the extended Freundlich isotherm model parameters; K_{F1} , K_{F2} , and n_1 and n_2 are also obtained from the corresponding mono-component Freundlich isotherm equations.

All multi-component isotherm model parameters were obtained by nonlinear regression employing the Excel software. The average

percentage errors (€%) between the experimental ($q_{eq,exp}$) and calculated ($q_{eq,calc}$) values were calculated for N , number of measurements, using the following equation:

$$(\%) = \frac{\sum_{i=1}^N |(q_{eq,i,exp} - q_{eq,i,calc}) / q_{eq,i,exp}|}{N} \times 100 \quad (10)$$

3.6 Application of mono-component adsorption models to equilibrium data

The equilibrium isotherms were obtained for the three mono-component (BB, BR, BY), three binary (BB-BY, BB-BR, BR-BY) and one ternary (BB-BR-BY) component systems and given in Fig. 8a-c. When the shapes of all obtained isotherms were classified according to Giles classification [44], it was seen that all isotherm shapes corresponds to the high affinity class (L and H type). In this situation, adsorption has a chemical character. This suggests that bentonite has a high affinity for these dyes in single and multi-solutions as an adsorbent and that there is no competition from solvent for adsorption sites. Similar results were obtained by Gonzales-Pradas et al. [45].

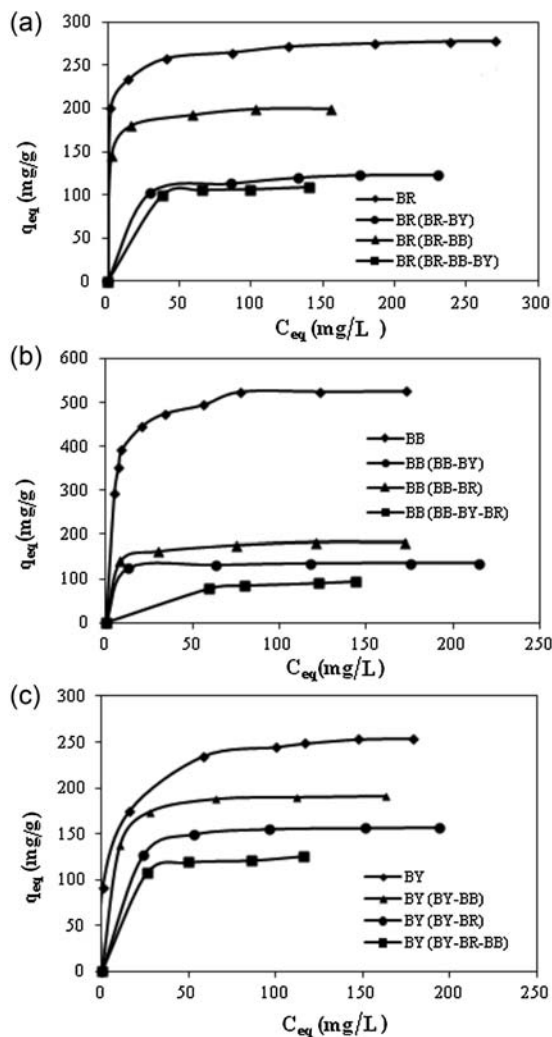


Figure 8. Nonlinear adsorption isotherms of dyes in single, binary and ternary solutions for (a) BR, (b) BB, and (c) BY.

The Langmuir and Freundlich adsorption isotherm models were applied to the adsorption data in single, binary, and ternary systems. The corresponding Freundlich and Langmuir parameters (q_{max} , K_F , n) and correlation coefficients (R^2) are given in Table 5. The results indicates that Langmuir and Freundlich models can be applied for BY, BR, and BB adsorption with high regression coefficients for single, binary, and ternary solutions of dyes onto bentonite, also better fit to the Langmuir model was obtained (all of $R^2 = 0.999$). The linearity of the Freundlich isotherm model slightly deviated (R^2 is in the range of 0.829–0.988). Also, we can evaluate that whether the nature of adsorption is either favorable or unfavorable by using the Freundlich parameters (K_F and n) [46]. When obtained n -value is $n < 1$ (S shape isotherm, concave profile), $n = 1$ (C shape isotherm curve), $n > 1$ (relatively slight slope), it indicates unfavorable adsorption, linear and favorable adsorption, respectively [46]. The BY, BR, and BB dye adsorption from the single, binary, and ternary solutions, the n values for the three systems studied fall in the range of 4.93–31.05, indicating that sorption intensity is favorable for the studied concentration range.

The bentonite showed an uptake capacity of 526 mg/g for BB followed by 278 mg/g for BR, and 256 mg/g for BY in single solutions (Table 5). The results in Table 5 clearly show the presence of other dyes decreasing the constant (K_F and q_{max}) values, which reflect the interference of competing dyes [16]. Generally, it is seen that the value of an individual dye adsorption capacity decreases in multi-dye systems but decreasing ratio varies with the type of the dye [20].

The equilibrium uptake of a dye in single and binary solution can be compared using the reduction of adsorption capacity for one dye in presence of the other dye at equilibrium. The reduction of dye ($R\%$) is the ratio of the difference between non-competitive (for single component) adsorption capacity (q_{max}) and competitive adsorption (for binary and ternary component) capacity ($q_{max,comp}$) to non-competitive adsorption, observed at equilibrium (Eq. (11)).

$$\text{Reduction (R)\%} = \frac{(q_{max} - q_{max,comp})}{q_{max}} \times 100 \quad (11)$$

The reduction of each dye in multi-component systems were calculated and obtained results given as:

- for BB dye: a reduction of 65, 74, and 79% in adsorption capacity was found in the order for BB-BR < BB-BY < BB-BR-BY, respectively.
- for BR dye: a reduction of 28, 54, and 60% in adsorption capacity was found in the order for BR-BB < BR-BY < BR-BB-BY, respectively.
- for BY dye: a reduction of 23, 37, and 49% in adsorption capacity was found in the order for BY-BB < BY-BR < BY-BR-BB, respectively.

These results also showed that BY dye is most dominant and BB is most recessive dye in multi dye systems. The values of $R\%$ also show that adsorption of BY, BR, and BB is suppressed by the presence of other dyes in solutions. For example for BB-BY binary system; the total adsorbed amount of each dye in single solutions is 782 mg/g (526 + 256 mg/g), but 333 mg/g (137 + 196 mg/g) in their binary solutions. The similar reductions were obtained for the other binary and ternary systems. Furthermore, bentonite's adsorption capacity for BY, BR, and BB decreases more in ternary versus binary systems. For example, while the total equilibrium uptakes of bentonite for BB, BR, and BY were 1060 mg/g in the single solute systems, it

Table 5. The Langmuir and Freundlich isotherms parameters for single, binary, and ternary dye systems

Dye system	Langmuir isotherm parameters			Freundlich isotherm parameters		
	q_{max} (mg/g)	K_a (L/mg)	R^2	K_F (mg/g) (mg/L) ^{1/n}	n	R^2
BB (single)	526.3	0.260	0.999	264.1	6.67	0.886
BB (BB-BR)	185.2	0.265	0.999	116.7	10.96	0.976
BB (BB-BY)	137.0	0.514	0.999	114.2	31.05	0.981
BB (BB-BY-BR)	108.7	0.042	0.999	34.2	4.93	0.988
BR (single)	277.8	0.319	0.999	195.3	15.33	0.972
BR (BR-BY)	128.2	0.114	0.999	73.9	10.39	0.977
BR (BR-BB)	200.0	0.575	0.999	138.7	12.80	0.949
BR (BR-BB-BY)	112.4	0.194	0.999	77.2	14.20	0.934
BY (single)	256.4	0.257	0.999	105.9	6.07	0.933
BY (BY-BR)	161.3	0.194	0.999	97.0	10.28	0.829
BY (BY-BB)	196.1	0.277	0.999	101.1	8.72	0.849
BY (BY-BB-BR)	131.6	0.178	0.999	80.1	10.45	0.935

was obtained as 353 mg/g for three dyes in the ternary system (Table 5). The decreasing of total adsorption capacity in multi-dye systems was also reported by Vinod and Anirudhan [19] and Choy et al. [47].

As a result, the presence of a second or a third dye decreased the adsorption capacity of an individual dye. A lot of reason can be consider to explain this reduced capacities; interaction between dyes in solution, competitive adsorption between dyes for active sites, change of the adsorbent surface charge, molecular size of adsorbent, pore size, and pore blockage [20, 21].

3.7 Application of multi-component adsorption models to equilibrium data

For multi-component isotherm modeling, modified Langmuir, SRS, and modified extended Freundlich isotherm models were used. The

experimental data obtained from the adsorption studies of BB-BY, BB-BR, and BY-BR binary solutions onto bentonite at a temperature 30°C and pH 6.0 have been applied to these three isotherm model equations. The multi-component isotherm parameters and equilibrium adsorption of BB, BY, and BR in binary solutions has been calculated by nonlinear regression from Eqs. (6) to (9), respectively, by minimizing standard deviations between the experimental and the calculated q_{eq} values. The calculated isotherm parameters from each isotherm model and percentage error values are presented in Table 6.

All the modified Langmuir coefficients, η_i and η_j , estimated for all binary dye system were $\ll 1.0$ indicating that mono-component Langmuir model should be corrected when applied to binary dye system. However, the use of the interaction terms, η_i and η_{ji} , in the modified Langmuir model not clearly decreased the error values

Table 6. Calculated error values and isotherms parameters for single and binary dye systems

Single dye	Langmuir isotherm				Freundlich isotherm			
	€ %				€ %			
BB	2.3				5.9			
BR	1.5				1.8			
BY	2.6				8.7			
Binary dye	Modified Langmuir isotherm				Langmuir isotherm			
	η_1	η_2	€ ₁ %	€ ₂ %	€ ₁ %	€ ₂ %		
BB(1)-BY(2)	0.0008	0.0002	17.5	2.9	12.4	6.9		
BB(1)-BR(2)	0.0029	0.0015	18.1	9.6	20.1	9.3		
BR(1)-BY(2)	0.0003	0.0001	13.0	6.4	12.3	9.1		
	SRS isotherm				Freundlich isotherm			
	θ_{12}	θ_{21}	€ ₁ %	€ ₂ %	€ ₁ %	€ ₂ %		
BB(1)-BY(2)	6.43	0.08	16.9	7.8	9.9	8.2		
BB(1)-BR(2)	3.04	0.32	12.4	5.0	10.2	8.3		
BR(1)-BY(2)	1.55	0.28	7.9	15.0	11.2	6.7		
Extended Freundlich isotherm								
	x_1	y_1	z_1	x_2	y_2	z_2	€ ₁ %	€ ₂ %
BB(1)-BY(2)	0.052	0.830	0.330	0.135	1.5×10^{-5}	1.946	8.4	3.9
BB(1)-BR(2)	0.476	1.094	0.620	0.694	0.143	0.843	6.5	3.9
BR(1)-BY(2)	0.809	4.005	0.598	0.006	0.010	0.762	2.8	4.1

when compared those of Langmuir isotherm models values. Namely, it can be said that the modified Langmuir model is not superior to Langmuir model for defining the all binary systems at this study. Several investigators have stated that the interaction factor (η) employed the model with only limited success [21, 48].

The SRS isotherm model equation (Eq. (7)) is a different version of the multi-component Freundlich type equation which theoretical principal of this model is that distribution of adsorption energies is exponential for each solute. The adsorption competition coefficient, θ_{ij} , describes the inhibition to the adsorption of component i by component j . The competition coefficients of the first and second dye component, θ_{12} and θ_{21} , were estimated from the competitive adsorption data of BB(1)-BY(2), BB(1)-BR(2), BR(1)-BY(2) binary systems. A comparison of the competition coefficients shows that the uptake of the BB dye that is more favorably adsorbed in single solutions was strongly affected by the presence of BY ($\theta_{12} = 6.43$), while the inhibition exerted in the reverse situation was less ($\theta_{21} = 0.08$). Similarly, it is also seen in Table 6, by the presence of BY (BR-BY binary systems) and BR (BB-BR binary system) affected the uptake of BR ($\theta_{12} = 1.55$) and BB ($\theta_{12} = 3.05$), respectively. The competition coefficients seem to prove that the adsorption of BB, BR, and BY dyes onto bentonite was inhibited by the presence of other dye. The SRS model was able to describe all three binary dye systems with low error values (%) within the ranges of 5.0–16.9%. The obtained SRS competitive coefficients also proved that the magnitude of BY competition over other dyes was significant (Table 6).

The extended Freundlich isotherm constants of the first and second dye were evaluated from model equations (Eqs. (8) and (9)) and given in Table 6. The obtained ϵ values showed that the extended Freundlich isotherm adequately well fits to equilibrium data of all dyes with the lowest error values in the range of 2.8–8.4% for binary dye systems. Comparison of error values obtained from Freundlich and extended Freundlich isotherm models for binary systems showed that the modification of Freundlich model equation to extended Freundlich equation gives superior results to model equilibrium of the binary adsorption system.

As a result, the modified Langmuir, SRS, and extended Freundlich isotherm models fitted reasonably well to the binary adsorption data of BB-BY, BB-BR, and BR-BY dye onto bentonite. However, it was seen that, the extended Freundlich isotherm model fitted best to the experimental data with the lowest error values.

4 Conclusions

The adsorption of BB, BR, and BY basic dyes was investigated in single, binary, and ternary solutions in this study. The XRF and SEM analyses showed that some exchangeable cations of bentonite exchanged with dye's cations; and typical lamellar structure image of bentonite changes with rather homogenous surface coated with dye after adsorption, respectively. The equilibrium studies showed that the adsorbed dye amount of a dye at equilibrium (q_{eq}) change with the presence of second or third dye in the adsorption medium. A competition between the dyes occurs for the active sites. But the competitive effect of each dye is different in the adsorption medium.

The shape of all isotherms was evaluated according to Giles [44] classification. The results demonstrated that the shape of all isotherms corresponds to the high affinity class and adsorption nature has a chemical character. The results of equilibrium model-

ing indicate that Langmuir and Freundlich models can be applied for BY, BR, and BB adsorption with high regression coefficients for single, binary, and ternary solutions of dyes onto bentonite, also better fit to the Langmuir model than Freundlich isotherm model. For the multi-component isotherm models, it was determined that the modified Langmuir model was not superior to mono-component Langmuir model for defining the all binary systems. The low error% values were obtained for SRS equation model within the ranges of 5.0–16.9%. The extended Freundlich isotherm adequately well fits to equilibrium data of all dyes with the lowest error values in the range of 2.8–8.4% for binary dye systems and the best isotherm model in all applied multi-component isotherm models. A two-factor D-optimal design combined with RSM was applied for the understanding and optimization of adsorption of binary dye systems on the bentonite surface from solution. The offered statistical approach fulfilled a critical analysis of the individual and simultaneous interactive influences of the independent variables (initial dye concentrations) on the adsorption process of binary dye systems. In competitive adsorption of all binary dye systems, observed a common result that the maximum q_{eq} value for a dye in binary system was obtained in the case of initial concentration of this dye was higher than the other. Looking at the values of individual or total q_{eq} , maximum values were obtained from the BB-BR binary system.

Acknowledgments

This research was supported by the Mersin University Scientific Research Project Unit (BAP-TBMYO (MT) 2007-1). Thanks to MEITAM for SEM, XRF and IR analysis.

The authors have declared no conflict of interest.

References

- [1] S. J. Allen, G. J. McKay, F. Porter, Adsorption Isotherm Models for Basic Dye Adsorption by Peat in Single and Binary Component Systems, *J. Colloid Interface Sci.* **2004**, *280*, 322.
- [2] B. Zohra, K. Aicha, S. Fatima, B. Nourredine, D. Zoubir, Adsorption of Direct Red 2 on Bentonite Modified by Cetyltrimethylammonium Bromide, *Chem. Eng. J.* **2008**, *136*, 295.
- [3] L. Sepulveda, F. Troncoso, E. Contreras, C. Palma, Competitive Adsorption of Textile Dyes Using Peat: Adsorption Equilibrium and Kinetic Studies in Monosolute and Bisolute Systems, *Environ. Technol.* **2008**, *29*, 947.
- [4] B. Mounir, M. N. Pons, O. Zahraa, A. Yaacoubi, A. Benhammou, Discoloration of a Red Cationic Dye by Supported TiO_2 Photocatalysis, *J. Hazard. Mater.* **2007**, *148*, 513.
- [5] N. Atar, A. Olgun, S. Wang, S. Liu, Adsorption of Anionic Dyes on Boron Industry Waste in Single and Binary Solutions Using Batch and Fixed-Bed Systems, *J. Chem. Eng. Data* **2011**, *56*, 508.
- [6] B. Tyagi, C. D. Chudasama, R. V. Jasra, Determination of Structural Modification in Acid Activated Montmorillonite Clay by FT-IR Spectroscopy, *Spectrochim. Acta, Part A* **2006**, *64*, 273.
- [7] A. S. Özcan, A. Özcan, Adsorption of Acid Dyes from Aqueous Solutions onto Acid-Activated Bentonite, *J. Colloid Interface Sci.* **2004**, *276*, 39.
- [8] G. Rytwo, S. Nir, L. Margulies, B. Casal, J. Merino, E. Ruiz-Hitzky, J. M. Serratos, Adsorption of Monovalent Organic Cations on Sepiolite: Experimental Results and Model Calculations, *Clays Clay Miner.* **1998**, *46*, 340.
- [9] L. Margulies, H. Rozen, A. Nir, Model for Competitive Adsorption of Organic Cations on Clays, *Clays Clay Miner.* **1988**, *36*, 270.

- [10] E. Bulut, M. Ozacar, A. Şengil, Adsorption of Malachite Green onto Bentonite: Equilibrium and Kinetic Studies and Process Design, *Microporous Mesoporous Mater.* **2008**, *115*, 234.
- [11] J. Madejova, FTIR Techniques in Clay Mineral Studies: Review, *Vib. Spectrosc.* **2003**, *31*, 1.
- [12] N. Boujelben, J. Bouzid, Z. Elouear, Adsorption of Nickel and Copper onto Natural Iron Oxide-Coated Sand from Aqueous Solutions: Study in Single and Binary Systems, *J. Hazard. Mater.* **2009**, *163*, 376.
- [13] K. Kadirvelu, J. Goel, C. Rajagopal, Sorption of Lead, Mercury and Cadmium Ions in Multi-Component System Using Carbon Aerogel as Adsorbent, *J. Hazard. Mater.* **2008**, *153*, 502.
- [14] N. Fiol, I. Villaescusa, M. Martinez, N. Miralles, J. Poch, J. Serarols, Sorption of Pb(II), Ni(II), Cu(II) and Cd(II) from Aqueous Solution by Olive Stone Waste, *Sep. Purif. Technol.* **2006**, *50*, 132.
- [15] M. Otero, F. Rozada, A. Moran, L. F. Calvo, A. I. Garcia, Removal of Heavy Metals from Aqueous Solution by Sewage Sludge Based Sorbents: Competitive Effects, *Desalination* **2009**, *239*, 46.
- [16] M. Prasad, H.-Y. Xub, S. Saxena, Multi-Component Sorption of Pb(II), Cu(II) and Zn(II) onto Low-Cost Mineral Adsorbent, *J. Hazard. Mater.* **2008**, *154*, 221.
- [17] F. A. A. Al-Rub, M. Kandah, N. Al-Dabaybeh, Competitive Adsorption of Nickel and Cadmium on Sheep Manure Wastes: Experimental and Prediction Studies, *Sep. Sci. Technol.* **2003**, *38*, 483.
- [18] D. Mohan, C. U. Pittman, Jr, P. H. Steele, Single, Binary and Multi-Component Adsorption of Copper and Cadmium from Aqueous Solutions on Kraft Lignin – a Biosorbent, *J. Colloid Interface Sci.* **2006**, *297*, 489.
- [19] V. P. Vinod, T. S. Anirudhan, Adsorption Behavior of Basic Dyes on the Humic Acid Immobilized Pillared Clay, *Water Air Soil Pollut.* **2003**, *150*, 193.
- [20] Y. Al-Degs, M. A. M. Khraisheh, S. J. Allen, M. N. Ahmad, G. M. Walker, Competitive Adsorption of Reactive Dyes from Solution: Equilibrium Isotherm Studies in Single and Multisolute Systems, *Chem. Eng. J.* **2007**, *128*, 163.
- [21] K. Vijayaraghavan, Y.-S. Yun, Competition of Reactive Red 4, Reactive Orange 16 and Basic Blue 3 during Biosorption of Reactive Blue 4 by Polysulfone-immobilized *Corynebacterium glutamicum*, *J. Hazard. Mater.* **2008**, *153*, 478.
- [22] S. S. Moghaddam, M. R. A. Moghaddam, M. Arami, Response Surface Optimization of Acid Red 119 Dye Adsorption by Mixtures of Dried Sewage Sludge and Sewage Sludge Ash, *Clean – Soil Air Water* **2012**, *40* (6), 652–660.
- [23] DyStar Company. *Product Catalogue*, DyStar, Singapore **2012**.
- [24] M. Turabik, H. Kumbur, Change in Some Physicochemical Properties of Unye/Ordu Bentonite with Acid Activation, *Earth Sciences, Cumhuriyet Univ. Bull. Faculty Eng.* **2002**, *19* (1), 1.
- [25] E. Eren, B. Afsin, Investigation of a Basic Dye Adsorption from Aqueous Solution onto Raw and Pre-Treated Bentonite Surfaces, *Dyes Pigm.* **2008**, *76*, 220.
- [26] M. J. Anderson, P. J. Whitcomb, *RSM Simplified: Optimizing Processes Using Response Surface Methods for Design of Experiments*, CRC Press Taylor & Francis Group, New York **2005**.
- [27] M. A. Bezerra, R. E. Santelli, E. P. Oliveria, L. S. Villar, L. A. Escalera, Response Surface Methodology (RSM) as a Tool for Optimization in Analytical Chemistry, *Talanta* **2008**, *76*, 965.
- [28] R. H. Myers, D. C. Montgomery, *Response Surface Methodology: Process and Product Optimization Using Designed Experiments*, 2nd Ed., John Wiley & Sons, Hoboken, NJ **2002**.
- [29] C. B. Ojeda, F. S. Rojas, Recent Developments in Derivative Ultraviolet/Visible Absorption Spectrophotometry, *Anal. Chim. Acta* **2004**, *518*, 1.
- [30] J. Karpinska, Derivative Spectrophotometry – Recent Applications and Directions of Developments, *Talanta* **2004**, *64*, 801.
- [31] J. A. Gadsden, *Infrared Spectra of Minerals and Related Inorganic Compounds*, Butterworths, London **1975**.
- [32] M. Mana, M. S. Ouali, L. C. de Menorval, Removal of Basic Dyes from Aqueous Solutions with a Treated Spent Bleaching Earth, *J. Colloid Interface Sci.* **2007**, *307*, 9.
- [33] Q. Li, Q.-Y. Yue, H.-J. Sun, Y. Su, B.-Y. Gao, A Comparative Study on the Properties, Mechanisms and Process Designs for the Adsorption of Non-Ionic or Anionic Dyes onto Cationic-Polymer/Bentonite, *J. Environ. Manage.* **2010**, *91*, 1601.
- [34] M. Toor, B. Jin, Adsorption Characteristics, Isotherm, Kinetics, and Diffusion of Modified Natural Bentonite for Removing Diazo Dye, *Chem. Eng. J.* **2012**, *187*, 79.
- [35] J. Zolgharnein, A. Shahmoradi, Adsorption of Cr(VI) onto *Elaeagnus* Tree Leaves: Statistical Optimization, Equilibrium Modeling, and Kinetic Studies, *J. Chem. Eng. Data* **2010**, *55*, 3428.
- [36] Z. Zhang, H. Zheng, Optimization for Decolorization of Azo Dye Acid Green 20 by Ultrasound and H₂O₂ Using Response Surface Methodology, *J. Hazard. Mater.* **2009**, *172*, 1388.
- [37] G. Barman, A. Kumar, P. Khare, Removal of Congo Red by Carbonized Low-Cost Adsorbents: Process Parameter Optimization Using a Taguchi Experimental Design, *J. Chem. Eng. Data* **2011**, *56*, 4102.
- [38] A. Özer, G. Gürbüz, A. Çalımlı, B. K. Körbahti, Biosorption of Copper(II) Ions on *Enteromorpha prolifera*: Application of Response Surface Methodology (RSM), *Chem. Eng. J.* **2009**, *146*, 377.
- [39] P. Sharma, L. Singh, N. Dilbaghi, Response Surface Methodological Approach for the Decolorization of Simulated Dye Effluent Using *Aspergillus fumigatus* Fresenius, *J. Hazard. Mater.* **2009**, *161*, 1081.
- [40] I. Langmuir, The Adsorption of Gases on Plane Surfaces of Glass, Mica and Platinum, *J. Am. Chem. Soc.* **1918**, *40*, 1361.
- [41] H. M. F. Freundlich, Over the Adsorption in Solution, *J. Phys. Chem.* **1906**, *57*, 385.
- [42] J. C. Bellot, J. S. Condoret, Modelling of Liquid Chromatography Equilibrium, *Process Biochem.* **1993**, *28*, 365.
- [43] Z. Aksu, D. Akpınar, Competitive Adsorption of Phenol and Chromium(VI) from Binary Solutions onto Dried Anaerobic Activated Sludge, *Biochem. Eng. J.* **2001**, *7*, 183.
- [44] C. H. Giles, D. Smith, A. Huitson, A General Treatment and Classification of the Solute Adsorption Isotherm, I. Theoretical, *J. Colloid Interface Sci.* **1974**, *47*, 755.
- [45] E. Gonzales-Pradas, M. Villafranca-Sanchez, F. Del Rey-Bueno, M. D. Urena-Amate, M. Socias-Viciana, M. Fernandez-Perez, Removal of Diquat and Deisopropylatrazine from Water by Montmorillonite-(Ce or Zr) Phosphate Crosslinked Compounds, *Chemosphere* **1999**, *39*, 455.
- [46] F. H. Frimmel, L. Huber, Influence of Humic Substances on the Aquatic Sorption of Heavy Metals on Defined Minerals Phases, *Environ. Int.* **1996**, *22*, 507.
- [47] K. K. H. Choy, S. J. Allen, G. McKay, Multi-Component Equilibrium Studies for the Adsorption of Basic Dyes from Solution on Lignite, *Adsorption* **2005**, *11*, 255.
- [48] K. K. H. Choy, J. F. Porter, G. McKay, Langmuir Isotherm Models Applied to the Multi-Component Sorption of Acid Dyes from Effluent onto Activated Carbon, *J. Chem. Eng. Data* **2000**, *45*, 575.